A novel role for microtubules in apoptotic chromatin dynamics and cellular fragmentation

David K. Moss*, Virginie M. Betin*, Soazig D. Malesinski‡ and Jon D. Lane§

Department of Biochemistry, University of Bristol, School of Medical and Veterinary Sciences, University Walk, Bristol, BS8 1TD, UK

*These authors contributed equally to this work

‡Present address: School of Pharmacy, Université de la Mediteranée, 27 Bd Jean Moulin, 13005 Marseille, France

§Author for correspondence (e-mail: jon.lane@bristol.ac.uk)

Accepted 24 February 2006
Journal of Cell Science 119, 2362-2374 Published by The Company of Biologists 2006
doi:10.1242/jcs.02959

Summary

Dramatic changes in cellular dynamics characterise the apoptotic execution phase, culminating in fragmentation into membrane-bound apoptotic bodies. Previous evidence suggests that actin-myosin plays a dominant role in apoptotic cellular remodelling, whereas all other cytoskeletal elements dismantle. We have used fixed cells and live-cell imaging to confirm that interphase microtubules rapidly depolymerise at the start of the execution phase. Around this time, pericentriolar components (pericentrin, ninein and γ-tubulin) are lost from the centrosomal region. Subsequently, however, extensive non-centrosomal bundles of densely packed, dynamic microtubules rapidly assemble throughout the cytoplasm in all cell lines tested. These microtubules have an important role in the peripheral relocation of chromatin in the dying cell, because nocodazole treatment restricts the dispersal of condensed apoptotic chromatin into surface blebs, and causes the withdrawal of chromatin fragments back towards the cell centre. Importantly, nocodazole and taxol are both potent inhibitors of apoptotic fragmentation in A431 cells, implicating dynamic microtubules in apoptotic body formation. Live-cell-imaging studies indicate that fragmentation is accompanied by the extension of rigid microtubule-rich spikes that project through the cortex of the dying cell. These structures enhance interactions between apoptotic cells and phagocytes in vitro, by providing additional sites for attachment to neighbouring cells.

Supplementary material available online at
http://jcs.biologists.org/cgi/content/full/119/11/2362/DC1

Key words: Apoptosis, Microtubules, Fragmentation, Chromatin, Live-cell imaging

Introduction

Apoptosis is a highly coordinated form of cell death that has vital roles in development and homeostasis in multicellular organisms (Kerr et al., 1972). Many human diseases (including some cancers) arise through inappropriate regulation of apoptosis, so a thorough understanding of this fundamental process is essential. Rapid progress has been made towards characterising the key apoptotic regulatory pathways (Strasser et al., 2000), at the hub of which are the caspases – cysteinyl proteases that are activated at the start of the execution phase, and cleave a sub-population of structural and regulatory proteins at conserved aspartic acid residues (Fischer et al., 2003). Henceforth, a series of predictable changes in cell behaviour takes place that distinguishes apoptosis from other classes of cell death (Mills et al., 1999). These changes are thought to be important for preparing dying cells for rapid and safe engulfment by phagocytes – a vital step in the apoptotic pathway in multicellular organisms.

Early during the execution phase, apoptotic cells pull away from their neighbours while undergoing a transient period of surface blebbing (Mills et al., 1999) that is dependent upon activation of myosin II via caspase cleavage of Rho-activated kinase (ROCK I) (Coleman et al., 2001; Sebbagh et al., 2001). Ultimately, apoptotic cells break up into membrane-bound fragments (apoptotic bodies) by a poorly characterised process, which requires actin in several cell types (Cotter et al., 1992). Apoptotic bodies (and the surface blebs that precede them) incorporate fragments of condensed chromatin and caspase-modified autoantigens (Casciola-Rosen et al., 1994; Cline and Radic, 2004; Leist and Jaattela, 2001), and although this ordered packaging is considered to be important for maintaining immune self-tolerance (Savill et al., 2002; White and Rosen, 2003), its mechanisms remain obscure. To facilitate the safe removal of apoptotic cellular remnants, specific markers are revealed at the surface (Savill and Fadok, 2000). These are poorly defined, although caspase-dependent flipping of phosphatidyl serine (PS) to the outer leaflet of the plasma membrane (Fadok et al., 1992; Martin et al., 1996) does play a key role in recognition and/or uptake by PS-receptor-expressing phagocytes (Fadok et al., 2000; Fadok et al., 1992; Hoffmann et al., 2001). Several other classes of phagocyte receptors – including members of the integrin family, scavenger receptors and lectins – have been implicated in apoptotic clearance in other contexts (Savill and Fadok, 2000), suggesting that significant redundancy exists in the recognition/engulfment process.

Evidence suggests that different fates await each of the cytoskeletal components of the cell during apoptosis: actin is reorganised and directs various execution-phase events (for a review, see Mills et al., 1999); intermediate filaments fragment

as a result of caspase cleavage of vimentin, desmin and acidic cytokeratin subunits (Byun et al., 2001; Caulin et al., 1997; Chen et al., 2003); caspase-6 cleavage of A-type lamins disassembles the nuclear lamina (Rao et al., 1996) upstream of nuclear fragmentation (Ruchaud et al., 2002); and microtubules break down early during the execution phase by an unknown mechanism (Bonfoco et al., 1996; Mills et al., 1998a; Mills et al., 1999). As microtubules are substrates for motor-based organelle and membrane trafficking (Lane and Allan, 1998), it can be assumed that destruction of the microtubule network would contribute to the assorted changes in membrane dynamics that are apparent within the apoptotic cell, e.g. Golgi fragmentation (Lane et al., 2002; Sesso et al., 1999) and secretory membrane traffic arrest (Lowe et al., 2004).

Chromatin-rich surface blebs are a hallmark of the late-apoptotic cell, and their formation requires actin-myosin II (Bonanno et al., 2000; Croft et al., 2005). However, we have recently described a potential role for microtubules in this process (Lane et al., 2005), and microtubules have now been observed in late-apoptotic HeLa cells (Lane et al., 2005), and in apoptotic CCRF-CEM cells (Pittman et al., 1997; Pittman et al., 1994). Here, we have used single-cell imaging to clarify the fate of microtubules in apoptosis, and to investigate further their roles in the dying cell. We found that the bulk of the interphase microtubule array disassembles at the onset of the execution phase as previously proposed (Mills et al., 1998a; Mills et al., 1999), concomitant with disruption of centrosomal architecture. However, these are soon replaced by extensive, dynamic bundles that perform three important roles: firstly, they contribute to the relocation of condensed chromatin into surface blebs; secondly, microtubules are required for cellular fragmentation; thirdly, by extending rigid cellular spikes, microtubules assist in tethering apoptotic cells to phagocytes.

Results

Microtubules are required for chromatin dispersal in late-apoptotic cells

A characteristic feature of late-apoptotic cells is the presence of large surface blebs that accumulate condensed chromatin. Our previous studies suggested a dominant role for actin-myosin II in this process, but provided evidence that microtubules might also be involved (Lane et al., 2005). Using confocal immunofluorescence microscopy, we have confirmed the presence of apoptotic microtubule arrays in all cell lines tested so far (e.g. HeLa, SW13.Cl-2, F111, A431 and NRK; this study and data not shown), treated with various inducers of apoptosis including UV, anisomycin, TNFα, Fas, TRAIL (this study and data not shown). The organisation of microtubules varied between individual apoptotic cells, but in all cases extensive bundles were observed extending into surface blebs in association with condensed chromatin (Fig. 1A and supplementary material Movie 1).

The apparent close association between microtubules and condensed chromatin in late-apoptotic cells prompted us to assess whether microtubules contribute to apoptotic chromatin remodelling. HeLa cells were induced into apoptosis by anisomycin treatment, and then incubated for 6 hours in the absence or presence of the actin poison, latrunculin A, or the microtubule-depolymerising drug, nocodazole. Cells were then fixed and DAPI stained, and the proportion of apoptotic cells (cleaved PARP positive; data not shown) with fragmented chromatin within surface blebs was assessed by fluorescence microscopy (Fig. 1B). The majority (65.2%) of apoptotic cells possessed chromatin-containing surface blebs (Fig. 1B), but this was dramatically reduced by nocodazole (25.8%; Fig. 1B). Latrunculin A had a much more pronounced effect, however (4.0% of apoptotic cells) (Fig. 1B), probably because actin poisons prevent plasma membrane blebbing (Mills et al., 1998b), and block chromatin budding from the nucleus (Bonanno et al., 2000; Croft et al., 2005) – events that must take place upstream of chromatin redistribution. These data suggest that microtubules and actin cooperate to drive apoptotic chromatin dispersal.

Microtubules could play a direct role in chromatin dispersal, or they might be more passive, in resisting some form of retractile pressure. To clarify this, we induced apoptosis by UV treatment, incubated cells for 4 hours to accumulate cells in apoptosis, and then for a further 40 minutes in the presence or absence of nocodazole (Fig. 1C). The proportion of apoptotic cells with dispersed versus compact chromatin was then assessed by fluorescence microscopy. Following nocodazole treatment, significantly fewer apoptotic cells possessed dispersed chromatin (Fig. 1C). This suggests that microtubule disruption allows chromatin to retreat back to the cell centre, but what retractile forces are acting here? Apoptotic surface blebbing is driven by myosin-II-actin contractility, initiated by caspase cleavage of ROCK I (Coleman et al., 2001; Sebbagh et al., 2001). Recent evidence suggests that in actively blebbing cells, myosin-II-driven contraction of newly assembled cortical actin bundles also cooperates with plasma membrane tension and extracellular osmotic forces to withdraw surface blebs (Charras et al., 2005). To assess whether microtubules resist the influence of similar retractile forces acting on peripheral chromatin, we tested latrunculin A and blebbistatin (a myosin II inhibitor) (Straight et al., 2003) in our assays (Fig. 1C). Addition of either drug individually caused a moderate shift from dispersed to compact chromatin (Fig. 1C), possibly because actin-myosin II drives the initial steps in chromatin dispersal (Bonanno et al., 2000; Croft et al., 2005). There were different outcomes, however, when these drugs were added in combination with nocodazole: a small additive affect was observed with latrunculin A and nocodazole, but blebbistatin and nocodazole together caused a shift towards compact chromatin that was comparable with data obtained using nocodazole alone (Fig. 1C). Hence, although actin somehow contributes to the retraction of chromatin into the cell centre when microtubules are absent, myosin II appears to be dispensable for this process.

The apoptotic microtubule array forms de novo during the execution phase

By assessing the status of the apoptotic microtubule array in HeLa cells at different stages of apoptosis (see Lane et al., 2002), we confirmed that microtubules are abundant within most early-apoptotic cells, and in the vast majority of late-apoptotic cells (Fig. 2). Interestingly, we could not detect microtubules in around half of the mid-apoptotic cells encountered (Fig. 2), with the remainder possessing very few intact microtubules (data not shown). Time-lapse phase-contrast and fluorescence microscopy of A431 cells transiently expressing YFP-tubulin and the chromatin marker, HMGB1-CFP (Lane et al., 2005), suggested that extensive

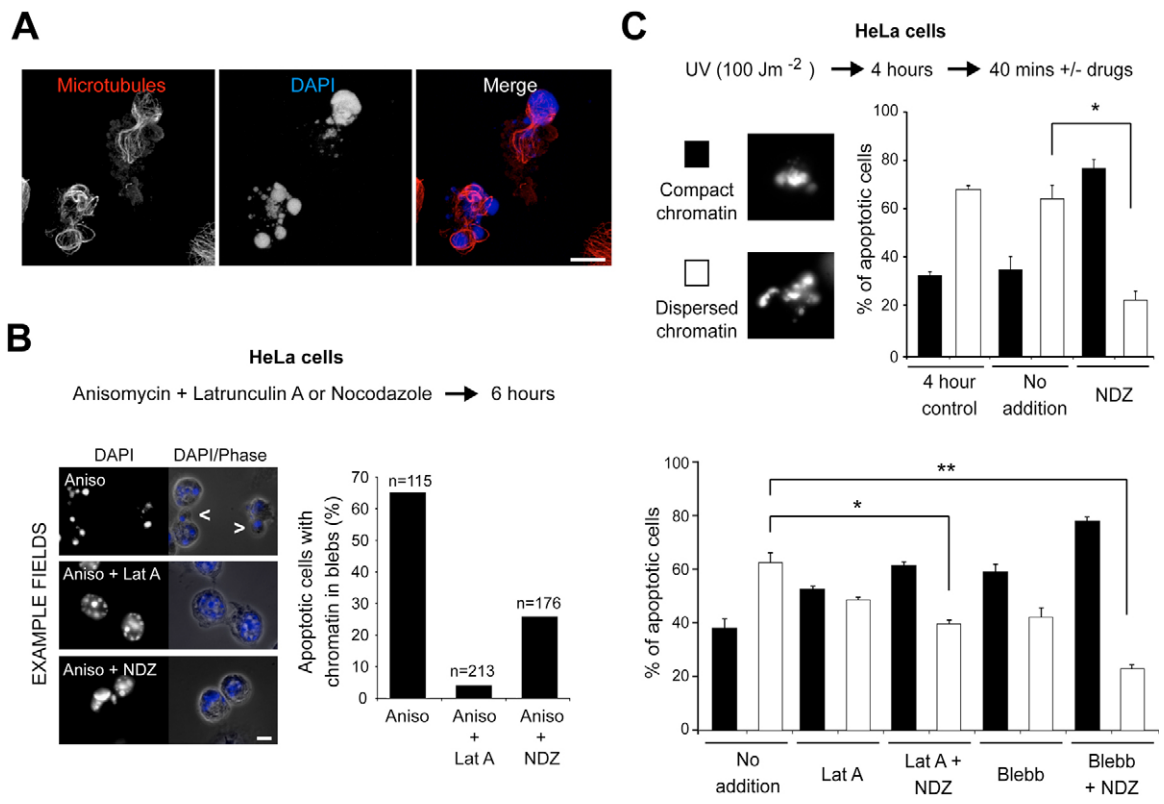

Fig. 1. Microtubule organisation in late-apoptotic HeLa cells. (A) Confocal image of apoptotic HeLa cells (6 hours anisomycin treatment) labelled with an anti-tubulin antibody (red) and DAPI (blue). Microtubules extend away from the body of the cell into chromatin-rich surface blebs. Bar, 10 μm. A Volocity 3-D reconstruction of the lower apoptotic cell is shown in supplementary material Movie 1. (B) Chromatin redistribution into surface blebs in apoptotic HeLa cells treated with anisomycin (Aniso, 6 hours) in the absence or presence of latrunculin A (Lat A) or nocodazole (NDZ). The proportion of apoptotic cells (cleaved PARP-positive, not shown) with condensed chromatin in surface blebs was then quantified after DAPI staining. Arrows in the images indicate chromatin-containing blebs. Bar, 10 μm. (C) Microtubules are required to maintain the dispersed status of condensed apoptotic chromatin. HeLa cells were induced into apoptosis by UV irradiation, incubated for 4 hours then for a further 40 minutes in the absence or presence of nocodazole, latrunculin A or blebbistatin (Blebb) (alone or in combination). Cells were fixed and assessed for compact or dispersed chromatin (cells defined as having dispersed chromatin contained three or more distinct, pyknotic pieces of peripheral chromatin, clearly distinguishable from the central mass; see example images). Values are mean ± s.e.m. Significant differences were observed where indicated, $^{**}P<0.001$ and $^{*}P<0.01$ using the Student's *t*-test.

depolymerisation of the interphase microtubule array takes place just before cell retraction (supplementary material Movie 2). Similar results were seen in apoptotic HeLa cells (data not shown). Together, these data suggest that the interphase microtubule network is disassembled early in the execution phase, as previously observed (Bonfoco et al., 1996; Mills et al., 1998a; Mills et al., 1999), but that it is replaced by an apoptotic microtubule array at later stages. In support of this, the majority of apoptotic microtubules were not recognised by antibodies to acetylated α-tubulin – a post-translational modification indicative of a long-lived polymer (Maruta et al., 1986) (supplementary material Fig. S1).

In healthy mammalian cells, microtubules grow from localised nucleation centres, most notably the centrosomes, however, the fate of this organelle during apoptosis remains undetermined. Live-cell imaging demonstrated that GFP-centrin-2 – a marker for the inner centriole (see Bornens, 2002) – persists into the late stages of apoptosis (Fig. 3A,B and supplementary material Movie 3). Interestingly, however, immunolabelling for the more peripheral, pericentriolar components, pericentrin, γ-tubulin and ninein (see Bornens, 2002), diminished during the early stages of the execution phase (Fig. 3A,B). Pericentrin labelling was maintained in the presence of zVAD.FMK, however, implicating caspases in this process (our unpublished results). Observations of centrosomal staining in relation to the progression of apoptosis (using the parameters defined in Fig. 2), suggested that γ-tubulin was lost from apoptotic centrosomes in early-to-mid apoptosis, implying that the breakdown of centrosomal integrity occurs concomitant with disassembly of the interphase microtubule network (compare Fig. 2 and Fig. 3C). Consequently, the apoptotic microtubule array is established later despite the lack of important components of the pericentriolar material. Whether the disrupted centrosome is capable of nucleating microtubules remains undetermined, however, confocal microscopy of late-apoptotic cells transiently expressing GFP-centrin suggested that the bulk of the apoptotic microtubules do not converge here (data not shown).

Microtubules are required for apoptotic cell fragmentation

Apoptotic cell fragmentation has previously been shown to

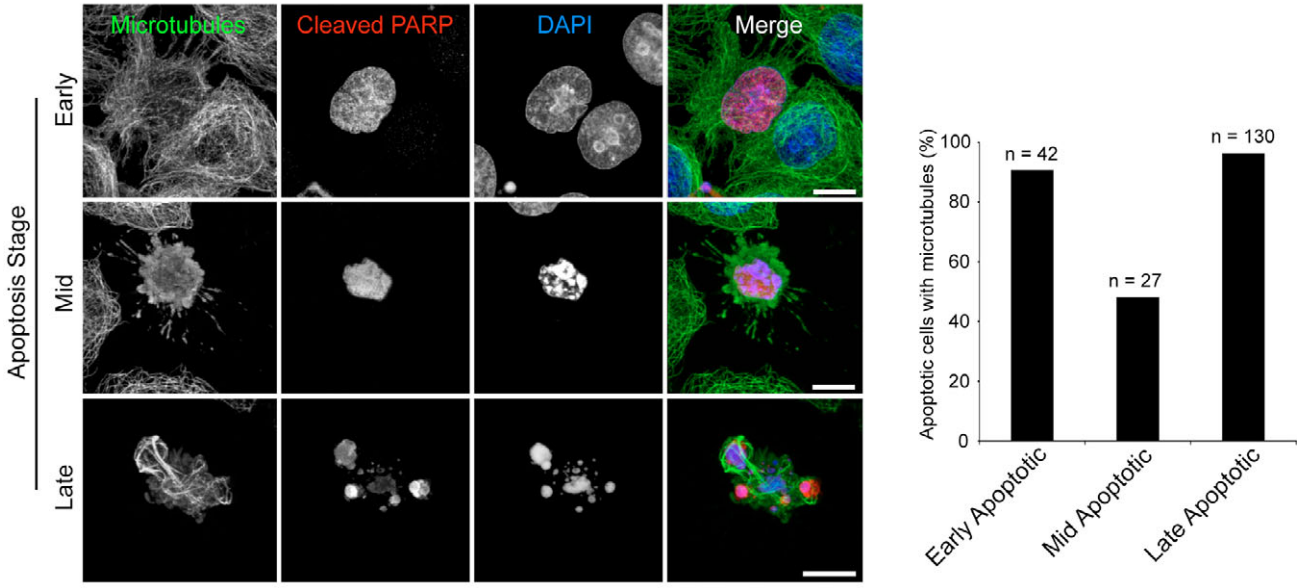

Fig. 2. Formation of the apoptotic microtubule array in mid-to-late apoptosis. To the right, the proportion of HeLa cells possessing microtubules at various stages of apoptosis, based on the morphological characteristics shown to the left (only cells completely lacking microtubules were scored as 'negative'). Anisomycin-treated HeLa cells were stained for microtubules (green), cleaved PARP (red) and DAPI (blue). Early-apoptotic cells have cleaved PARP, but no evidence of chromatin condensation. In mid-apoptotic cells, cleaved PARP-positive nuclei are still intact but display evidence of chromatin condensation. By late apoptosis, chromatin is fragmented and dispersed. Bars, 10 μm.

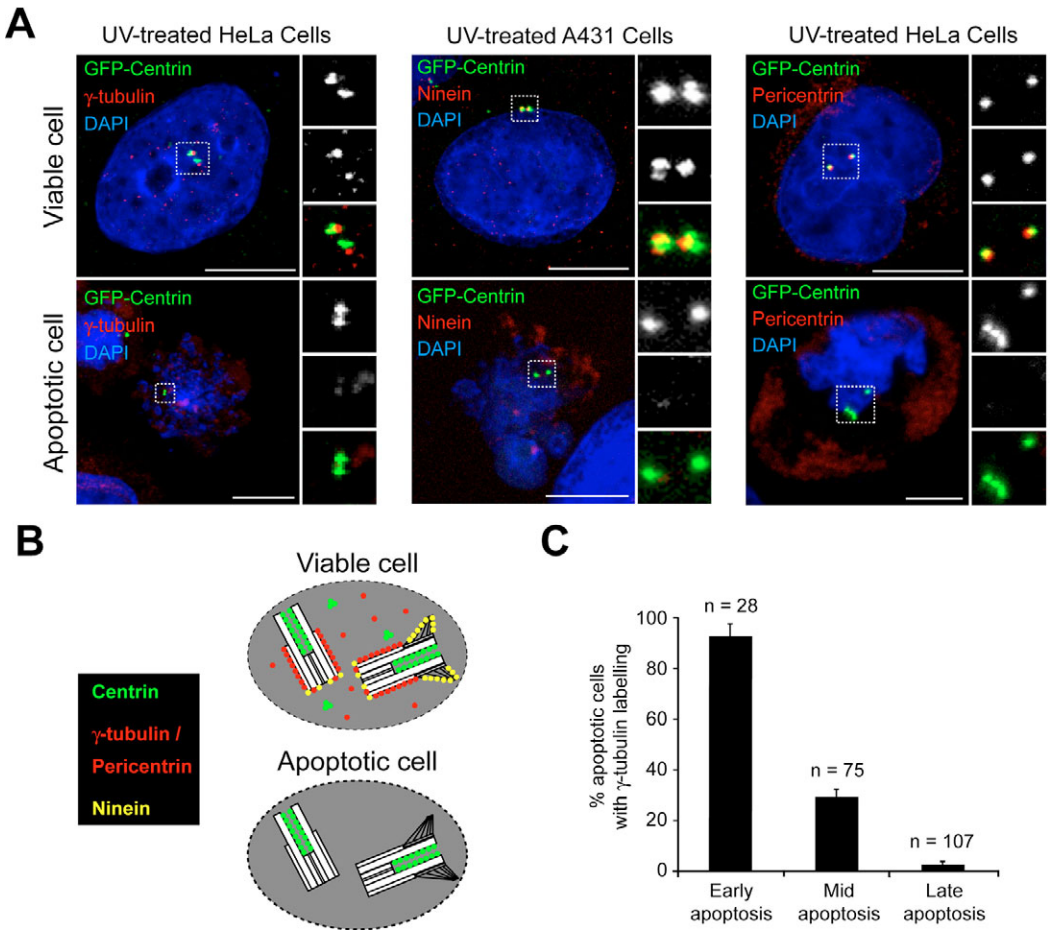

Fig. 3. Effects of apoptosis on centrosome integrity. (A) Confocal maximum projections of viable and apoptotic cells transiently expressing GFP-Centrin 2 and subsequently labelled with antibodies against γ-tubulin, ninein or pericentrin. In each zoomed panel to the right of the main image, GFP-centrin labelling is to the top, γ-tubulin, ninein or pericentrin in the middle, with the merged image in the bottom panel. Bars, 5 μm. (B) Cartoon showing the relative locations of each of the centrosomal markers in A, adapted from Bornens (Bornens, 2002) with permission. The grey region around the centrioles represents the pericentriolar space. (C) Quantification of the mean percentage (± s.e.m.) of apoptotic HeLa cells (UV treated) positive for γ-tubulin labelling. Apoptosis stage was determined using the morphological criteria described in Fig. 2.

require actin (Cotter et al., 1992) and myosin II (Coleman et al., 2001). To examine whether microtubules also play a role, we first set out to identify a cell line that undergoes apoptotic fragmentation in vitro with physiological kinetics (i.e. around the time of PS exposure: ~2 hours post cell release) (see Lane et al., 2005). Unlike other cell lines that we analysed (e.g. HeLa, NRK, Jurkat, SW13 and HL60) that underwent only minimal fragmentation during this brief period (data not shown), A431 cells produced multiple apoptotic bodies in response to diverse apoptotic stimuli. Hence, we have used this cell line for our fragmentation studies. UV-irradiated A431 cells were incubated for 8 hours in the absence or presence of the microtubule poisons nocodazole and taxol, the ROCK I inhibitor Y27632 and the caspase inhibitor zVAD.FMK. Analysis of caspase (DEVDase) activity and PARP cleavage (Fig. 4A) suggested that apoptosis rate was elevated a little in the presence of Y27632, however, neither of the microtubule inhibitors significantly affected DEVDase activity in apoptotic A431 cells (although PARP cleavage was slower in taxol-treated cells) (Fig. 4A).

We tested the effect of cytoskeletal drugs on apoptotic fragmentation by two independent approaches: (1) by counting the number of <5 μm cell fragments released (Fig. 4B); (2) by FACs analysis to determine the proportion of cells with a sub-G1 DNA content (Fig. 4C; values for UV-only-treated cells were normalised to 100%). In both assays, nocodazole and taxol significantly reduced cell fragmentation, whereas Y27632 had no effect (Fig. 4B,C). As expected, fragmentation was blocked by zVAD.FMK, confirming that this is a caspase-dependent process (Fig. 4B,C). These results suggest that apoptotic body formation depends upon a functional microtubule cytoskeleton in A431 cells. Actin has previously been implicated in apoptotic fragmentation (Cotter et al., 1992). We therefore measured the affect of actin disruption in UV-treated A431 cells, but found no significant influence on fragmentation (although PARP cleavage was marginally elevated; Fig. 4D-F). Taken together, these data suggest that microtubules are important for apoptotic body formation in the A431 cell line, with actin-myosin playing less of a role.

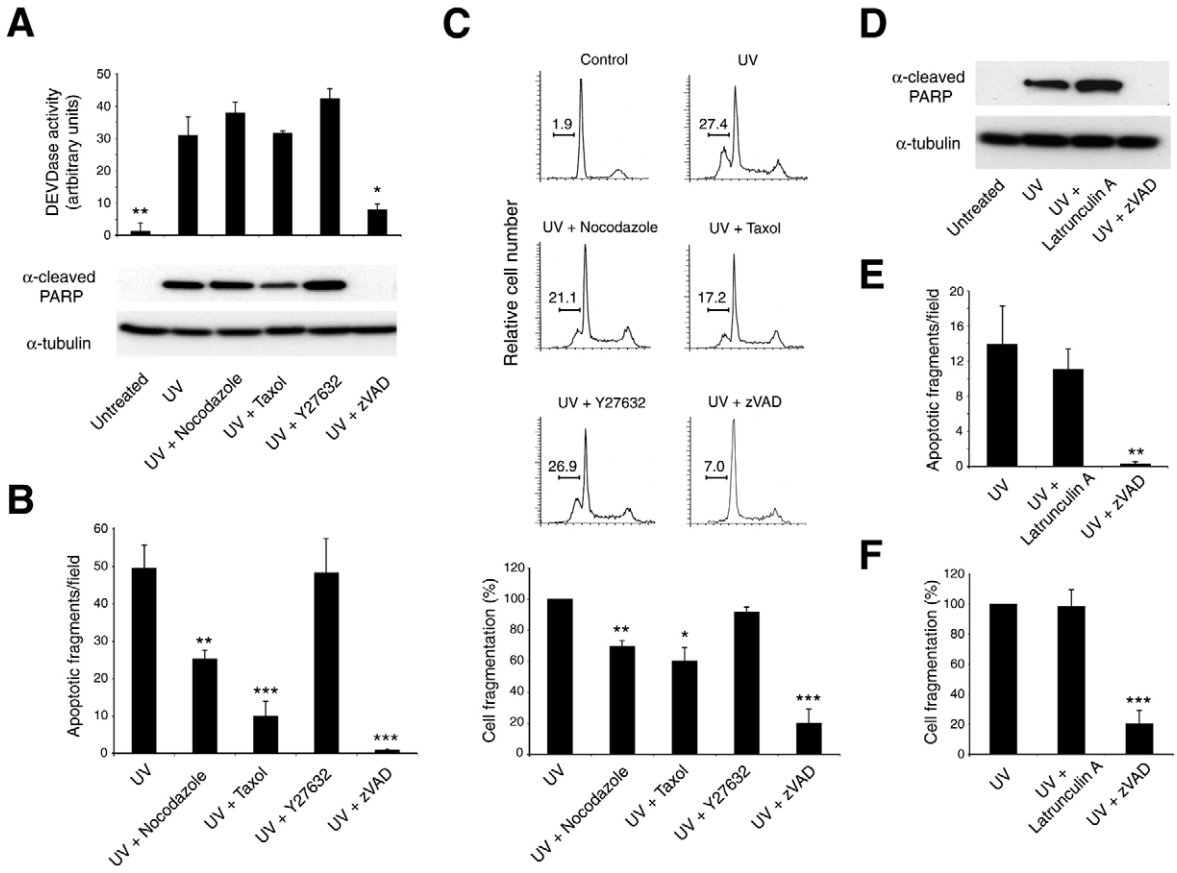

Fig. 4. Microtubules are required for apoptotic cell fragmentation. (A) Influence of cytoskeletal inhibitors on apoptotic progression in UV-treated A431 cells, measured using the fluorogenic caspase substrate, Ac.DEVD.AMC (top) and by immunoblotting for cleaved PARP (bottom: tubulin shown as a loading control). Mean values (± s.e.m.) are shown from triplicate assays. (B) Assessment of apoptotic body formation in UV-treated A431 cells. Sub-5-μm apoptotic A431 cell fragments were collected by filtration and were counted by fluorescence or phase-contrast microscopy. Experiments were performed blind and are the mean ± s.e.m. of three experiments. (C) FACs analysis of apoptotic fragmentation. The relative numbers of UV-irradiated A431 cells with sub-G1 DNA content is shown in the bar chart (bottom) as a function of the value for UV only treated cells (normalised to 100%). Values are from three independent experiments (example traces are shown). (D-F) The effect of Latrunculin A on apoptotic progression (D, PARP cleavage), cellular fragmentation by apoptotic body assay (E), and FACS (F). Statistical significance by Student's *t*-test in A,B,C,E,F: **P*<0.5; ***P*<0.01; ****P*<0.001 compared with levels in the UV-alone group.

Formation of apoptotic spikes during fragmentation in A431 cells

To try to clarify the role of microtubules in the A431 cell apoptotic fragmentation process, we monitored the execution phase by time-lapse phase-contrast microscopy. As with other cell types (Lane et al., 2005), partial release of A431 cells from the substratum was accompanied by dynamic surface blebbing lasting about 40 minutes (supplementary material Fig. S2A and Movie 4). Subsequently, cells entered the fragmentation phase, which in A431 cells was accompanied by formation of fine cellular projections or spikes that typically grew in excess of 20 μm (supplementary material Fig. S2A,C and Movie 4). Apoptotic bodies often remained attached to spikes, and as a result, apoptotic A431 cells adopted highly irregular profiles. Inclusion of fluorescent annexin V in the assay demonstrated that PS exposure occurs ~20-30 minutes after the appearance of the first spikes (data not shown). Importantly, nocodazole treatment blocked spike formation (supplementary material Fig. S2B,C and Movie 5), although the early execution phase (cell rounding and blebbing) was indistinguishable from control cells (compare supplementary material Movies 4 and 5). By comparison, inhibitors of actin-myosin had only a partial effect on spike formation: relatively few, highly elongated spikes were formed per cell in the presence of latrunculin A and Y27632, whereas blebbistatin supported the formation of numerous, fine, 'feathery' spikes (supplementary material Fig. S2C). In the presence of taxol, one or two much thicker spikes were produced, but these were clearly abnormal (supplementary material Fig. S2C). These observations suggest that there might be a functional correlation between the microtubule-dependent formation of apoptotic spikes and cell fragmentation. Interestingly, surface spikes were often observed in apoptotic SW13.Cl-2 cells, and were seen, albeit infrequently, in apoptotic HeLa and Jurkat cells. They are also a characteristic feature of apoptotic Meg01 cells (supplementary material Fig. S3), suggesting that they may be widespread.

Characterisation of the apoptotic microtubule array in A431 cells

Next, we carried out immunofluorescence microscopy of cytospin preparations of floating, apoptotic A431 cells labelled with anti-tubulin antibodies, phalloidin and DAPI (Fig. 5A-C). Microtubules were observed in all apoptotic cells, extending from the body of the cell into slender spikes (Fig. 5A,B). Apoptotic bodies remained attached along the lengths of spikes, or in clusters at their tips, and these contained loops of microtubules and often also fragments of condensed chromatin (Fig. 5A-C). Interestingly, phalloidin staining revealed that f-actin is also present in these structures (Fig. 5A-C), co-aligning with microtubules (Fig. 5B',C). We also noted the presence of apoptotic bodies dispersed between the intact cells. These often contained fragmented chromatin and cleaved PARP, and labelled strongly for cortical rings of

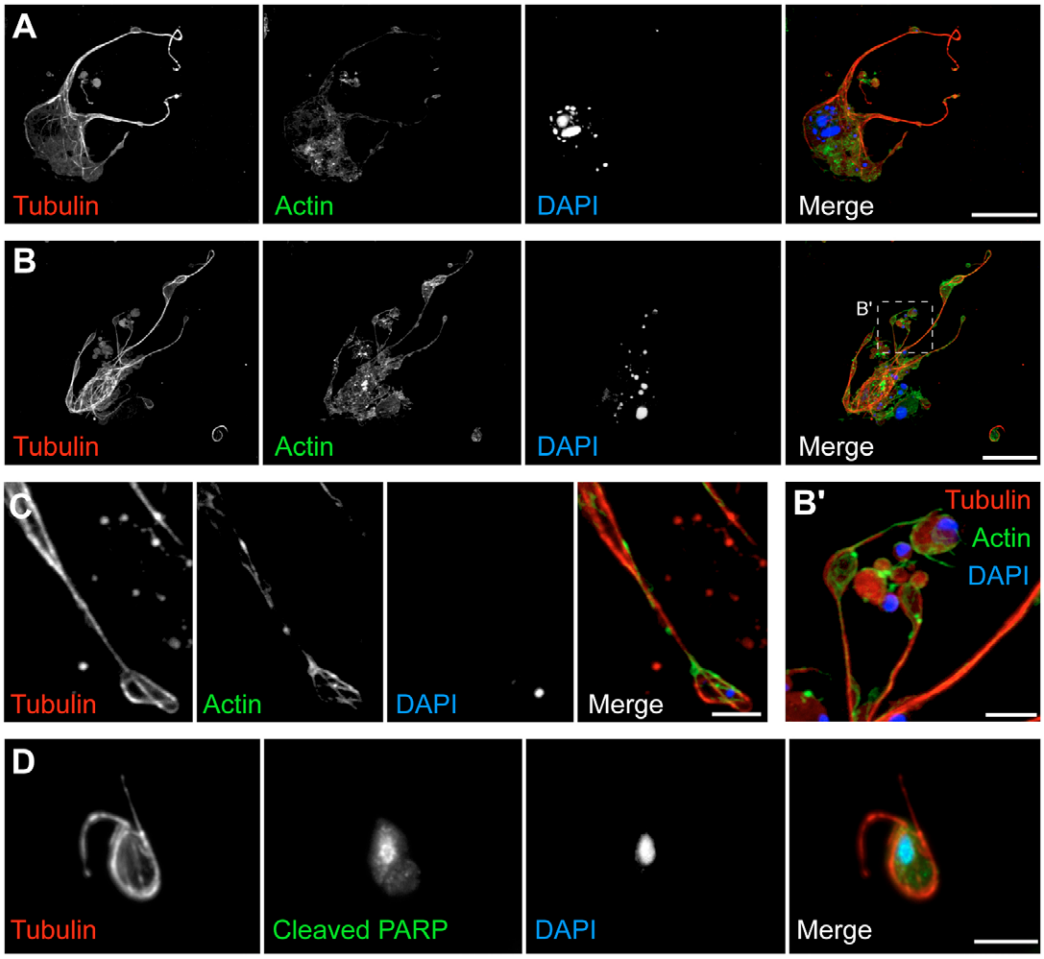

Fig. 5. Fluorescence microscopy of microtubule and actin distribution in apoptotic A431 cells. Confocal (A-C) and wide-field (D) fluorescence images of cytospin preparations of floating, UV-irradiated apoptotic A431 cells. (A,B) Apoptotic cells labelled with phalloidin (F-actin; green), anti-tubulin antibody (red) and DAPI (blue). (B') Detail of a cluster of apoptotic bodies formed at the tip of two spikes from the boxed region of the panel above. (C) Actin and microtubules co-align in apoptotic spikes. The body of the cell is located to the top left. (D) An isolated apoptotic body labelled for tubulin (red), cleaved PARP (green) and DAPI (blue). Bars, 10 μm (A,B); 2 μm (B',C); 5 μm (D).

microtubules (Fig. 5D), perhaps indicative of a structural role within apoptotic bodies.

Long-term time-lapse imaging of anisomycin-treated A431 cells, transiently co-expressing YFP-tubulin and HMGB1-CFP, confirmed that most interphase microtubules depolymerise shortly before cell rounding (Fig. 6A,B and supplementary material Movie 6). However, these are soon replaced by extensive bundles of unfocussed microtubules that assemble towards the cell periphery as cells begin retracting (Fig. 6A,B and supplementary material Movie 6). Subsequently, YFP-tubulin positive apoptotic spikes assemble, and clumps of condensed chromatin often remained associated with these peripheral structures (Fig. 6A,C and supplementary material Movie 6). To examine these structures in greater detail, we carried out TEM of floating, apoptotic A431 cells. In the cell body we identified patches of intersecting bundles of closely packed, linear protein filaments (Fig. 7A). The widths of these filaments were consistent with the diameter of microtubules in longitudinal section (22.76±1.38 nm; n=10), and they were regularly spaced at around 12.8 nm (n=8). Identical bundles of microtubules were observed extending into apoptotic spikes (Fig. 7B), where mitochondria and packages of condensed chromatin were often found in close proximity to microtubule bundles (Fig. 7B-D). In transverse sections of apoptotic spikes, microtubule profiles could clearly be identified (Fig. 7E,F).

One possible role for the apoptotic microtubule array is to provide a platform for directed (motor-based) transport within the dying cell. To investigate the orientation and dynamics of apoptotic microtubules, we labelled apoptotic A431 cells with an antibody recognising the microtubule plus-end-tracking P protein, EB1 (Su et al., 1995). EB1 tracks along growing microtubule tips, and is localised to the extreme plus ends of microtubules at steady state (Morrison et al., 1998). In fixed, apoptotic A431 cells, EB1 staining was coincident with microtubule tips, particularly towards the ends of apoptotic spikes (Fig. 8A). Time-lapse imaging revealed that EB1-GFP puncta (Morrison et al., 2002) continue to track with a subset of microtubules in apoptotic A431 cells, with movement almost exclusively away from the cell body (Fig. 8B and supplementary material Movie 7), suggesting that they are

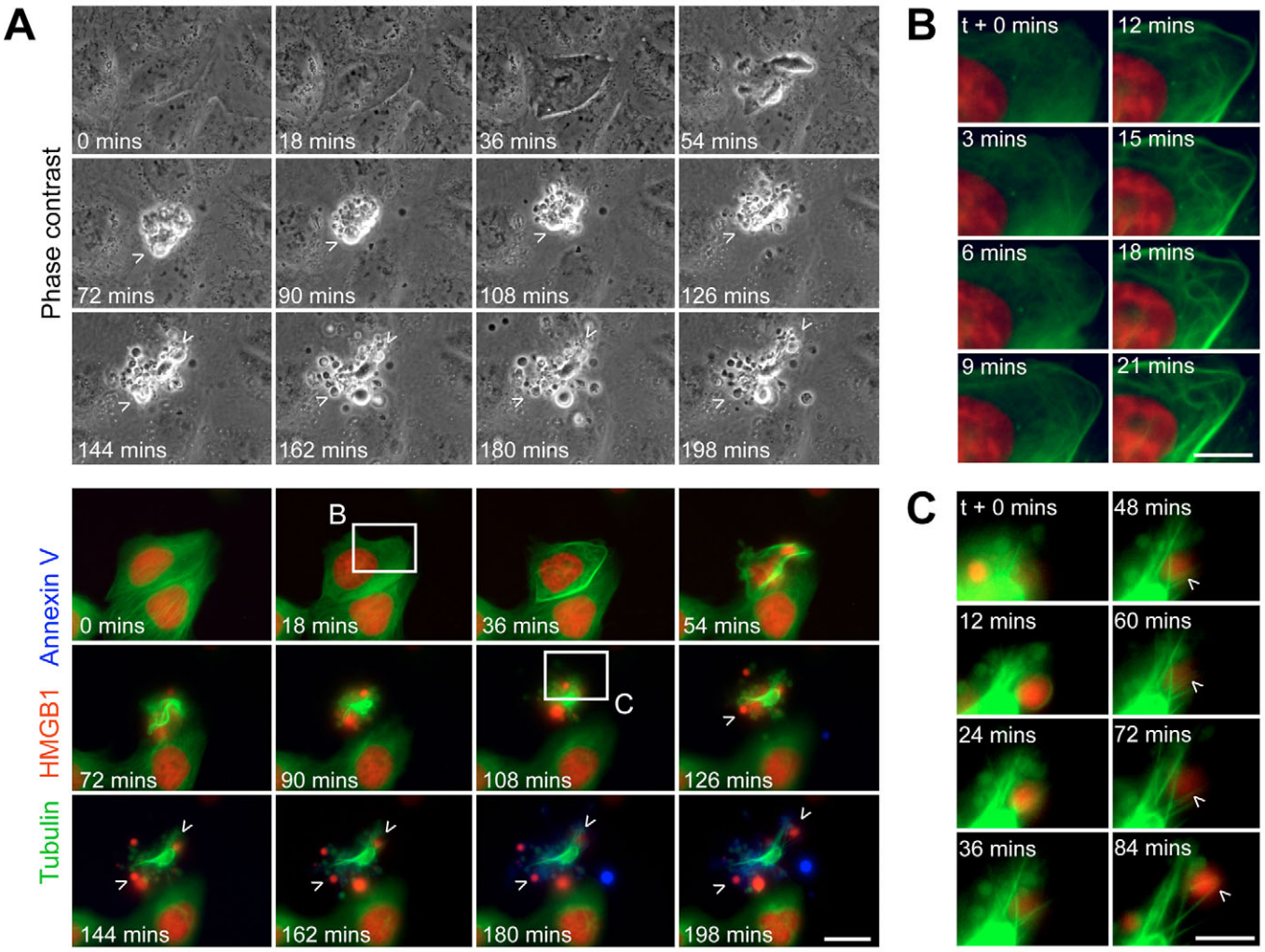

Fig. 6. Microtubule and chromatin dynamics in apoptotic A431 cells. (A) Time-lapse imaging of anisomycin-treated A431 cells transiently co-expressing YFP-tubulin (green) and HMGB1-CFP (red). Alexa Fluor 594-Annexin V labelling is false-coloured blue. Fluorescence frames are from supplementary material Movie 6. Bar, 20 μm. (B,C) Zoomed areas from the boxed regions indicated in A showing increased temporal resolution (annexin V channel omitted). Arrowheads indicate packets of condensed chromatin. Bar, 10 μm.

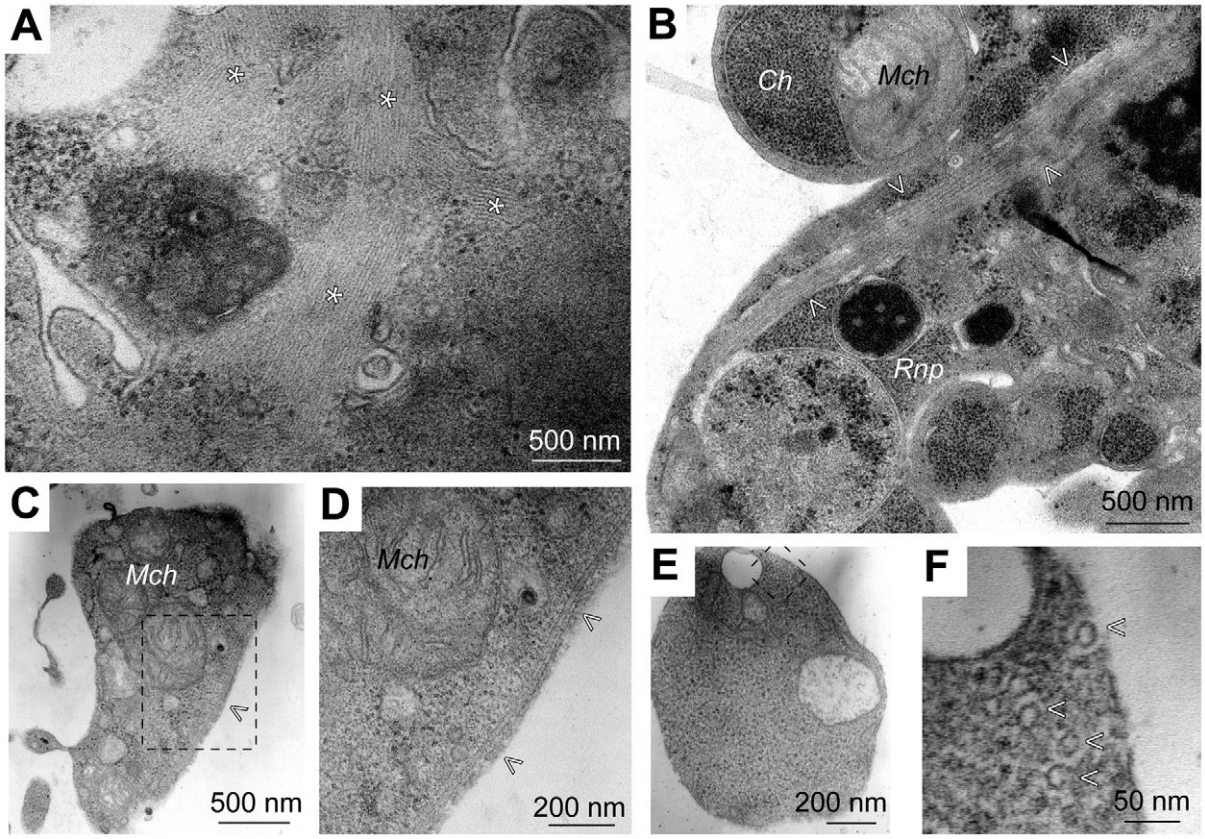

Fig. 7. TEM analysis of microtubule organisation in apoptotic A431 cells. (A) Bundles of closely packed, intersecting microtubules (asterisks) seen in longitudinal section (LS) in the body of an apoptotic A431 cell. (B) Detail of an area of cytoplasm at the base of an apoptotic spike. A bundle of microtubules (arrowheads) can be seen in LS running into the spike. Intact mitochondria (*Mch*), chromatin (*Ch*), ribonucleoprotein granules (*Rnp*) and unidentified membrane-bound organelles are also apparent. (C) A microtubule (arrowheads) running parallel to the plasma membrane of an isolated cell fragment is shown in close-up in D. (E) Transverse section through an apoptotic spike. Microtubule profiles can be seen in the close-up of the boxed area (arrows in F). In each example, apoptosis was induced by UV irradiation.

dynamic and predominantly plus ends outwards. To confirm the dynamic nature of these arrays, we carried out FRAP analysis upon apoptotic spikes in A431 cells stably expressing YFP-tubulin (Fig. 8C). In bleached regions, recovery of fluorescence was rapid, supporting the notion that apoptotic microtubules are dynamic (Fig. 8C). The rate of EB1-GFP movement was slow in apoptotic spikes (2-3 μm/minute, Fig. 8B and supplementary material Movie 7), in comparison with published microtubule growth rates in healthy cells (e.g. 5.8-7.0 μm/minute in PtK1 cells) (Wittmann et al., 2003), and we are currently investigating the reasons for these kinetic differences.

Apoptotic spikes enhance interactions with macrophages

The terminal phase of apoptosis in most tissues is phagocytosis. Since apoptotic spikes effectively increase cell surface area, we tested their influence upon binding and uptake by phagocytes. CellTracker-labelled A431 cells were induced into apoptosis by UV irradiation in the absence or presence of nocodazole, then incubated with THP-1 macrophages. In the absence of spikes (nocodazole treatment), the proportion of macrophages interacting with and engulfing apoptotic targets was markedly reduced compared with wild-type apoptotic cells (Fig. 9A). When we inspected the relationships between apoptotic target cells and macrophages, we observed that control apoptotic cells were typically bound to the surface of macrophages via apoptotic spikes (Fig. 9B,C). Notably, apoptotic bodies distributed along the lengths of the spikes acted as prominent sites for interaction (see zoomed panels in Fig. 9B,C). Phagocytosis markers are believed to accumulate upon surface blebs and apoptotic bodies (e.g. Casciola-Rosen et al., 1996; Ogden et al., 2001), thereby stimulating rapid recognition and engulfment. Our imaging studies suggest that spikes might assist this process by passively 'presenting' apoptotic bodies to phagocytes, and this is likely to account for the increased binding and engulfment activity observed in the phagocytosis assays.

Discussion

The execution phase of apoptosis is a highly coordinated process of cellular reorganisation that culminates in the packaging of chromatin into fragments (apoptotic bodies) that express surface 'eat-me' flags and are rapidly engulfed by phagocytes. The dramatic changes in cell behaviour that accompany the execution phase (i.e. release and retraction, blebbing and fragmentation) require an active cytoskeleton (see Mills et al., 1999), and a variety of studies have highlighted a role for actin-myosin in each of these steps

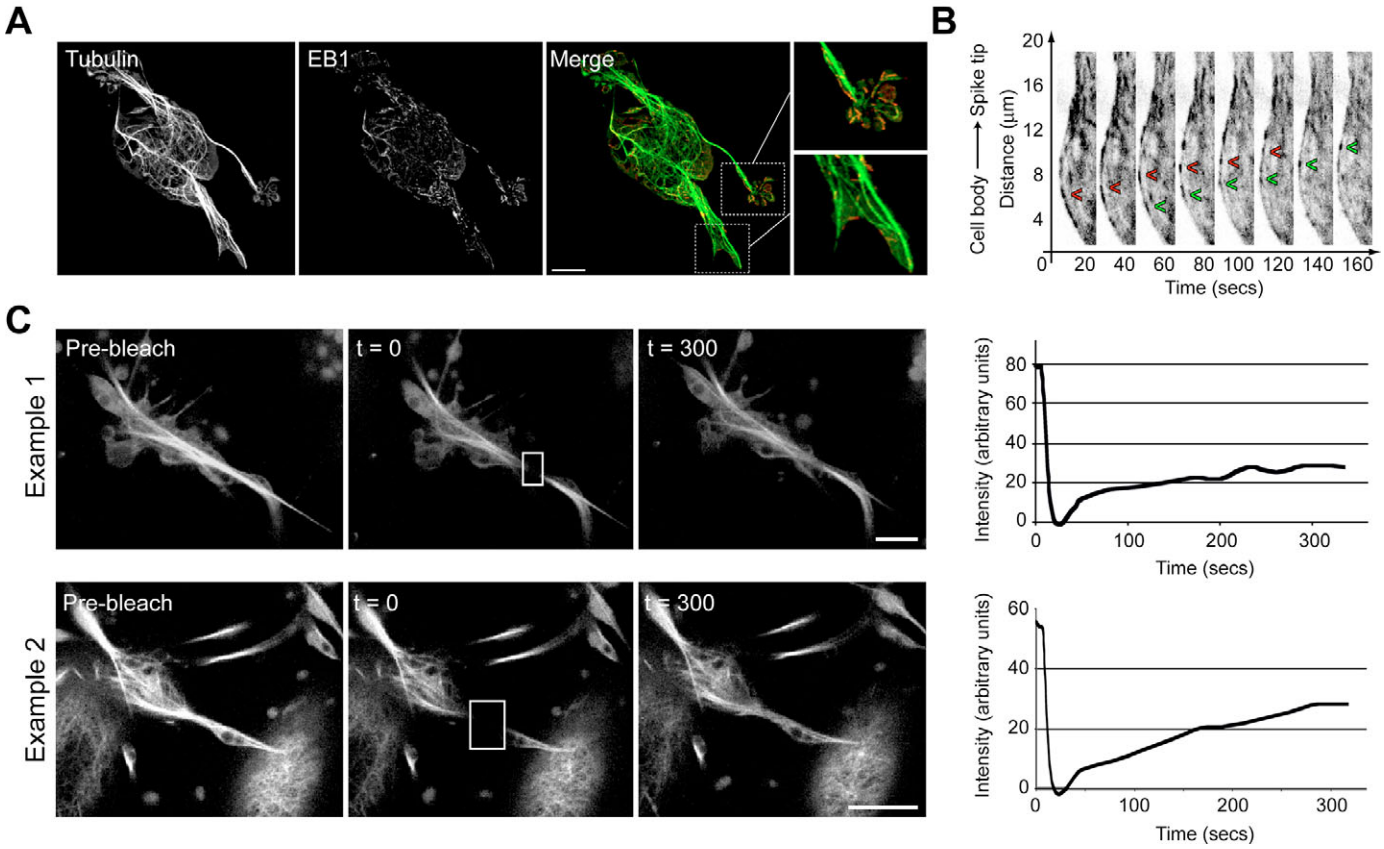

Fig. 8. Orientation and dynamics of apoptotic microtubules. (A) Confocal immunofluorescence imaging of EB1 distribution in an apoptotic A431 cell. EB1 puncta (red) are localised to the distal tips of microtubules (green) within apoptotic spikes. The boxed areas of the merge image are shown in close-up to the right. Bar, 10 μm. (B) Kymograph derived from a time-lapse sequence of EB1-GFP dynamics in an apoptotic A431 cell spike (supplementary material Movie 7). Puncta (arrows) move towards the spike tip. (C) FRAP analysis of microtubule polymer turnover in apoptotic spikes. Frames represent images of apoptotic spikes from A431 cells stably expressing YFP-tubulin, before and after photobleaching (boxed areas). To the right, quantification of fluorescence recovery in the boxed region. Bar, 10 μm.

(Bonanno et al., 2000; Coleman et al., 2001; Cotter et al., 1992; Croft et al., 2005; Sebbagh et al., 2001). Here, we have used fixed and live-cell imaging to show that microtubules are also common features of apoptotic cells. Significantly, we have demonstrated functions for apoptotic microtubules in chromatin repositioning and in apoptotic body formation (see supplementary material Fig. S4), implying that the role of the cytoskeleton in coordinating apoptotic cell remodelling is more complex than previously thought.

Formation of the apoptotic microtubule network is a biphasic process: first, during the early (release) phase, interphase microtubules rapidly dismantle, but these are soon replaced by extensive bundles of closely packed, new polymer. The microtubule depolymerisation phase correlated with the loss of peripheral centrosomal γ-tubulin, suggesting that the two events may be linked. Notably, although the core centrioles remain essentially intact throughout apoptosis (as judged by continued labelling with GFP-centrin 2; Fig. 3A and supplementary material Movie 3), they are unlikely to direct the formation of the novel microtubule array, because this is not assembled in a radial fashion, and instead appears randomly throughout the peripheral cytoplasm (see Fig. 6C and supplementary material Movie 6). The mechanisms responsible for centrosome disruption, and indeed for initial microtubule disassembly, remain undetermined. One possibility is that certain pericentriolar proteins are cleaved by caspases, but to our knowledge none has been identified as a caspase target (Fischer et al., 2003; Gerner et al., 2000). Interestingly, it has been demonstrated that the minus-end-directed motor, cytoplasmic dynein, is essential for the centrosomal localisation of pericentrin and γ-tubulin in healthy cells (Young et al., 2000). Cytoplasmic dynein function is arrested during the execution phase by caspase cleavage of the intermediate chains (Lane et al., 2001), so one possible explanation is that this reduces the concentration of pericentrin and γ-tubulin at the centrosome, thereby abrogating its capacity to nucleate microtubules. The mechanisms that control reassembly of microtubules later in the execution phase also remain uncertain, although it has recently been demonstrated that caspases can cleave the C-terminus of α-tubulin, thereby increasing its capacity to assemble into polymers (Adrain et al., 2006). We are currently investigating the potential links between α-tubulin cleavage and microtubule dynamics during apoptosis.

Prolonged nocodazole treatment blocked the accumulation of condensed chromatin in surface blebs during the apoptotic execution phase in HeLa cells. This finding could be explained either by microtubules playing a direct role in

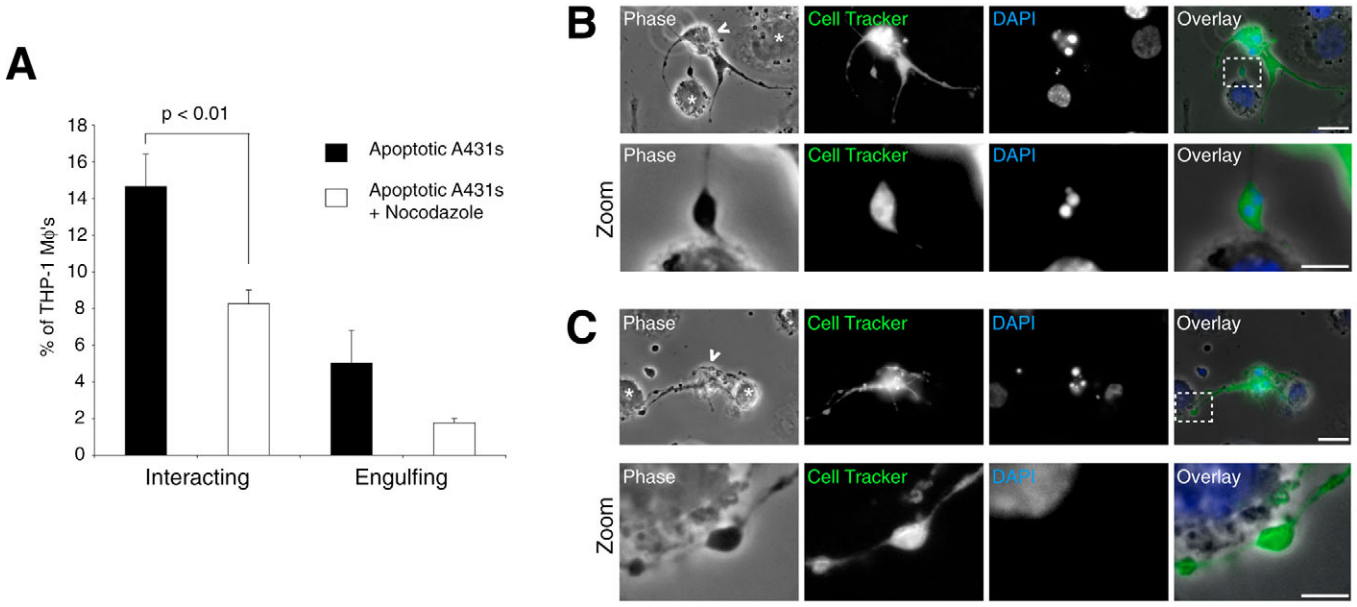

Fig. 9. Spikes enhance interaction between apoptotic cells and phagocytes. (A) Proportion of THP-1 macrophages interacting (bound and engulfed) and engulfing apoptotic A431 cells. Target cells were generated in the absence or presence of nocodazole. Shown are means (± s.e.m.) of triplicate samples from a single representative experiment (statistical analysis by Student's *t*-test). (B,C) Wide-field images of CellTracker-labelled apoptotic A431 cells (arrowheads) interacting with THP-1 macrophages (asterisks). Zoomed images of the boxed areas are shown in the bottom panels of B and C. Bars=10 μm (zoom=5 μm).

transporting chromatin towards the cell surface, and/or by microtubules acting to maintain the peripheral location of chromatin against retractile forces. Although we cannot rule out the former explanation, the fact that just a brief (40 minute) nocodazole treatment of apoptotic cells caused withdrawal of chromatin back towards the cell centre suggests that microtubules probably resist some form of retractile pressure. Contractility generated by actin and active myosin II is the best candidate here – it is believed to provide the cortical squeezing forces that drive apoptotic surface blebbing (Coleman et al., 2001; Mills et al., 1998b; Mills et al., 1999; Sebbagh et al., 2001), and it deforms the nuclear envelope to allow chromatin budding (Croft et al., 2005; Lane et al., 2005). Importantly, recent evidence from actively blebbing, non-apoptotic cells suggests that contraction of newly-assembled actin-myosin II cables just beneath the plasma membrane is also required to withdraw surface blebs, in combination with plasma membrane tension and extracellular osmotic pressure (Charras et al., 2005). Hence, paradoxically, the same contractile forces appear to be required for the establishment of chromatin-rich surface blebs (Lane et al., 2005), and subsequently also for bleb retraction (Charras et al., 2005). The tensegrity model for cytoskeletal function in cell morphogenesis explores the possibility that microtubules act as rigid struts against contractile actin-myosin forces to facilitate cell shape changes (see Rodriguez et al., 2003). We propose that the extensive bundles of microtubules that assemble during mid-to-late apoptosis can resist actin-myosin-II-mediated contractility, and thereby help to maintain the peripheral distribution of chromatin in the blebbing apoptotic cell. In support of this, chromatin dispersal assays highlighted a role for actin in chromatin coalescence when microtubules are depolymerised, although perhaps surprisingly, we were unable to demonstrate a requirement for myosin II in this process.

One of the final events in the execution phase is fragmentation into apoptotic bodies. In the majority of cell lines that we tested, this was a slow, passive process, becoming apparent long after the dynamic period of the apoptotic execution phase had ended – an observation also previously made by Mills et al. (Mills et al., 1999). One obvious exception was the A431 cell line, which underwent rapid apoptotic fragmentation that was always accompanied by the formation of long, microtubule-rich spikes. Our data showed that microtubules play an essential role in apoptotic body formation in this cell line, and we speculate that the ability to extend spikes might predispose a particular cell type to undergo regulated apoptotic fragmentation downstream of actin-driven surface blebbing. Coincident with the elongated bundles of microtubules, apoptotic spikes also contained filamentous actin. Although our data imply that actin is not essential for spike assembly, those produced in the absence of F-actin were typically fatter and were always unbranched. This suggests that actin and microtubules cooperate to an extent in late-apoptotic A431 cells, and that their continued interplay is important for apoptotic morphogenesis. Owing to our previous lack of appreciation of the presence of an apoptotic microtubule array (see Mills et al., 1999), the roles of actin-microtubule crosslinking proteins during apoptosis remain largely unexplored, although some are known to be caspase targets (including APC, cytoplasmic dynein/dynactin, plectin) (see Fischer et al., 2003). A regulatory link between microtubules and actin in the apoptotic cell may be RhoA, which coordinates actin and microtubule dynamics and/or stability via ROCK and the diaphanous-related formin, mDia, respectively (Palazzo et al., 2001; Rodriguez et al., 2003). Importantly, however, the

RhoA signalling pathway that coordinates actin fibre length and myosin II activity is short-circuited during apoptosis by caspase cleavage and activation of the RhoA effector, ROCK I (Coleman et al., 2001; Sebbagh et al., 2001), suggesting that this regulatory crossroads may be redundant in the dying cell.

A paradigm for microtubule-based cellular fragmentation is the terminal phase of thrombopoiesis, when megakaryocytes extend microtubule-rich proplatelets that bud to release platelets (Italiano, Jr et al., 1999). Microtubules run along the lengths of proplatelets, coiling at their tips to delineate the boundaries of nascent platelets, and are essential for proplatelet formation and platelet release (Hartwig and Italiano, Jr, 2003; Italiano, Jr et al., 1999). Significantly, budding occurs by a form of compartmentalised apoptosis (Clarke et al., 2003; De Botton et al., 2002), suggesting that this might be a functional adaptation of apoptotic body formation. The two processes do differ in several respects, however: firstly, apoptotic bodies carry condensed chromatin and are cleared rapidly (within hours) by phagocytes, whereas platelets actively exclude chromatin and have a life-span in circulation of about 7 days (Hartwig and Italiano, Jr, 2003); secondly, caspase activity within the megakaryocyte is restricted to the cell body as a result of exclusion of caspase-9 from proplatelets (Clarke et al., 2003), whereas active caspase-3 can be detected throughout apoptotic A431 cells (data not shown); finally, platelet formation is dependent upon the expression of haematopoietic β1-tubulin (Lecine et al., 2000), but this isoform could not be detected in immunoblots of apoptotic A431 cells (data not shown).

Evidence suggests that apoptotic cells are important reservoirs for autoantigens (see Rosen and Casciola-Rosen, 2001) that accumulate, with chromatin, within apoptotic surface blebs (e.g. Casciola-Rosen et al., 1994). However, the mechanisms regulating their peripheral localisation remain obscure. Our findings raise the prospect that microtubules might be involved in the coordinated transport of substrates such as these within apoptotic cells. Indeed, they might even provide a platform for the delivery of phagocytosis markers to the cell surface. Exposure of PS on the outer plasma membrane leaflet is generally accompanied by the appearance of altered glycoproteins and oxidised ligands that are thought to enhance the specificity of phagocyte recognition (Savill and Fadok, 2000). Whether microtubules are required for directed transport of proteins/lipids to the surface of apoptotic cells – which have profound defects in secretion (Lowe et al., 2004) – remains undetermined, but this would require sustained activity of microtubule motors. Caspase cleavage of the intermediate chain of the predominant minus end-directed motor, cytoplasmic dynein, and the $p150^{glued}$ component of its membrane adaptor, dynactin (Lane et al., 2001), probably excludes a role for this motor. Interestingly, our data suggest that the bulk of apoptotic microtubules are oriented plus end ‘outwards’, as is the case in healthy fibroblasts (Lane and Allan, 1998), so inhibition of minus-end-directed motors might be sufficient to bias traffic towards the cell periphery. The influence of caspase activity upon the function of other microtubule motors awaits clarification.

The generation of apoptotic bodies is considered to be an important step in the safe clearance of apoptotic corpses – they incorporate immunogenic substrates and improve the dispersal of the dying cell. Our data show that microtubules contribute to the process of apoptotic body formation by helping to sustain the peripheral localisation of chromatin within surface blebs, and by facilitating cell fragmentation. The mode of action of the apoptotic microtubule array and, in particular, whether microtubule motors play any role in the assembly and/or function of the apoptotic microtubule array – perhaps even by coordinating movement of cargoes within the dying cell – are the focus of future research in our laboratory.

Materials and Methods

Reagents

Unless otherwise stated, reagents were obtained from Sigma (Poole, UK). Stock solutions of anisomycin (5 mg/ml), nocodazole (5 mg/ml), taxol (paclitaxel™, Calbiochem, Nottingham, UK; 20 mM), zVAD.FMK (Calbiochem; 50 mM), Ac-DEVD.AMC (Calbiochem; 10 mM), Y27632 (Calbiochem; 100 mM), Propidium Iodide (20 mg/ml), RNaseA (15 mg/ml), DAPI (4′,6-diamidino-2-phenylindole; 1 mg/ml), latrunculin A (Molecular Probes, Eugene, OR; 10 mM) and blebbistatin (Calbiochem; 100 mM) were stored at –20°C. Alexa Fluor 594-annexin V, Alexa Fluor 488-phalloidin and CellTracker green (CMFDA; 10 mM) were obtained from Molecular Probes.

Antibodies

The following antibodies were used: monoclonal anti-tubulin (B5-1-2; Sigma); polyclonal anti-cleaved PARP (Promega, Southampton, UK); monoclonal anti-tyrosinated α-tubulin (YL1/2; from John Kilmartin, Cambridge, UK); monoclonal anti-acetylated α-tubulin (C3B9) and polyclonal anti-pericentrin, both from Peter March (Manchester, UK); monoclonal anti-EB1 (Transduction Labs); polyclonal anti-ninein (from Mette Mogensen, UEA, UK) (Baird et al., 2004).

Constructs

The human high-mobility-group box 1 (HMGB1)-YFP construct has been described (Lane et al., 2005). HMGB1-CFP was generated by subcloning into pECFP-N1 (Clontech). YFP-tubulin was obtained from Clontech. EB1-GFP was from the Morrison lab (University of Leeds, UK) (Morrison et al., 2002). Human GFP-Centrin 2 (White et al., 2000) was obtained from Jeff Salisbury (Mayo Clinic College of Medicine, MN). Transient transfections were carried out using Fugene 6 (Roche, Lewes, UK) according to the manufacturer’s instructions.

Cell lines

Cells were maintained either in DMEM (A431, HeLa, SW13.Cl-2) or RPMI (Meg01, Jurkat, HL60, THP-1) each containing 10% foetal bovine serum, at 37°C and 5% CO_2. A431 cells stably expressing YFP-tubulin were obtained following transient transfection by selecting positive clones after G418 treatment (Lane et al., 2002). THP-1 cells (ECACC, Salisbury, UK) were differentiated into macrophages by incubating for 72 hours with 240 nm PMA (phorbol 12-myristate 13-acetate).

Apoptosis induction and drug treatments

Cells were induced into apoptosis by treatment with 5 μg/ml anisomycin or by UV irradiation (100 Jm^{-2}) (Lane et al., 2002). Inhibitors were used at the following final concentrations: latrunculin A (1.0 μM); Y27632 (100 μM); blebbistatin (12.5 μm); nocodazole (5 μg/ml); taxol (20 μM); zVAD.FMK (50 μM).

Fluorescence microscopy and live-cell imaging

Wide-field fluorescence images were obtained using an Olympus IX-71 inverted microscope (60× Uplan Fluorite objective 0.65-1.25 NA, at maximum aperture) fitted with a CoolSNAP HQ CCD camera (Photometrics, Tucson, AZ) driven by MetaMorph software (Universal Imaging Corporation, Downington, PA). Confocal images were obtained using a Leica AOBS SP2 microscope (63× PLAPO objective 1.4 NA) at 0.2 μm *z*-steps. For immunofluorescence, cells were fixed in 2% paraformaldehyde (PFA: methanol-free, EM grade; TAAB, Aldermaston, UK) with 0.2% glutaraldehyde (TAAB), followed by permeabilisation with 0.1% Triton X-100, or in –20°C methanol. To analyse apoptotic spikes by immunofluorescence, floating apoptotic A431 cells were spun on to poly-L-lysine coated coverslips (using a Shandon cytospin 3: 1000 rpm, 5 minutes).

Live-cell imaging was carried out using the Olympus IX-71 system. Halogen lamp illumination was used for both transmitted light and for epifluorescence to extend cell viability (Lane et al., 2002). Cells were maintained in CO_2-independent DMEM (Invitrogen, Paisley, UK), at 37°C in 3 cm cell-imaging dishes (MatTek, Ashland, MA). FRAP investigations of YFP-tubulin-expressing apoptotic cells were carried out using the Leica AOBS SP2 confocal microscope.

Analysis of apoptosis and cellular fragmentation

UV-irradiated A431 cells were incubated for 8 hours in the absence or presence of inhibitors. Apoptosis was assessed by measuring Ac.DEVD.AMC fluorescence in

cell lysates (according to the manufacturer's instructions). In parallel experiments, A431 cells were processed for immunoblotting using anti-cleaved PARP and anti-tubulin antibodies. To quantify apoptotic bodies, CellTracker-green-labelled A431 cells were fixed by adding a one-third volume of 6% PFA to the culture medium, and passed through a 5 μm pore filter (Millipore, Watford, UK) by gravity flow (Cline and Radic, 2004). Apoptotic cell fragments were cytospun on to poly-L-lysine-coated coverslips as described above. The number of fragments in ten random fields was assessed, in triplicate, in blind experiments by fluorescence and phase-contrast microscopy. For flow cytometry, cells were fixed in ice-cold 70% ethanol, then incubated with 20 μg/ml Propidium Iodide in the presence of 15 μg/ml RNaseA for 1 hour at 37°C before being analysed using a FACScan (Becton Dickinson). Cellular fragmentation was expressed as the percentage of cells with sub-G1 DNA content.

Phagocytosis assays

PMA-differentiated THP-1 monocytes were adhered to glass coverslips in six-well plates (750,000 cells/well). CellTracker-labelled apoptotic A431 cells were irradiated then incubated for 8 hours in the absence or presence of 5 μM nocodazole. Floating apoptotic cells were washed and 120,000 cells were added to the THP-1 culture in 1 ml serum-free DMEM. After 30 minutes of co-incubation at 37°C, coverslips were washed extensively in PBS, and cells fixed in 2% PFA. The number of THP-1 macrophages interacting (bound and engulfed) and engulfing cell fragments was calculated in ten random fields in triplicate by fluorescence and phase-contrast microscopy.

Electron microscopy

Apoptotic A431 cells were obtained by aspiration of culture medium from a dish of UV-irradiated cells, fixed by adding an equal volume of 4% glutaraldehyde, then processed for transmission electron microscopy as described previously (Lane et al., 2005).

We acknowledge the support of the Medical Research Council in providing an Infrastructure Award to establish the School of Medical Sciences Cell Imaging Facility at Bristol University. We are grateful to Debbie Carter and Ginnie Tilly for assistance with EM, to Helena Patsos for FACS, to Nick Cowan (NYU Medical Centre) for the β1-tubulin antiserum, and to Marko Radic (Tennessee Health Services Centre, USA) for sharing the apoptotic body filtration assay pre-publication. Thanks also to Harry Mellor, David Stephens and Ruth Rollason for critical reading of the manuscript. This work is supported by a Wellcome Trust Research Career Development Fellowship to J.D.L. (No. 067358), and a Wellcome Trust Project Grant (No. 074208).

References

Adrain, C., Duriez, P. J., Brumatti, G., Delivani, P. and Martin, S. J. (2006). The cytotoxic lymphocyte protease, granzyme B, targets the cytoskeleton and perturbs microtubule polymerization dynamics. *J. Biol. Chem.* **281**, 8118-8125.

Baird, D. H., Myers, K. A., Mogensen, M., Moss, D. and Baas, P. W. (2004). Distribution of the microtubule-related protein ninein in developing neurons. *Neuropharmacology* **47**, 677-683.

Bonanno, E., Ruzittu, M., Carla, E. C., Montinari, M. R., Pagliara, P. and Dini, L. (2000). Cell shape and organelle modification in apoptotic U937 cells. *Eur. J. Histochem.* **44**, 237-246.

Bonfoco, E., Leist, M., Zhivotovsky, B., Orrenius, S., Lipton, S. A. and Nicotera, P. (1996). Cytoskeletal breakdown and apoptosis elicited by NO donors in cerebellar granule cells require NMDA receptor activation. *J. Neurochem.* **67**, 2484-2493.

Bornens, M. (2002). Centrosome composition and microtubule anchoring mechanisms. *Curr. Opin. Cell Biol.* **14**, 25-34.

Byun, Y., Chen, F., Chang, R., Trivedi, M., Green, K. J. and Cryns, V. L. (2001). Caspase cleavage of vimentin disrupts intermediate filaments and promotes apoptosis. *Cell Death Differ.* **8**, 443-450.

Casciola-Rosen, L. A., Anhalt, G. and Rosen, A. (1994). Autoantigens targeted in systemic lupus erythematosus are clustered in two populations of surface structures on apoptotic keratinocytes. *J. Exp. Med.* **179**, 1317-1330.

Casciola-Rosen, L., Rosen, A., Petri, M. and Schlissel, M. (1996). Surface blebs on apoptotic cells are sites of enhanced procoagulant activity: implications for coagulation events and antigenic spread in systemic lupus erythematosus. *Proc. Natl. Acad. Sci. USA* **93**, 1624-1629.

Caulin, C., Salvesen, G. S. and Oshima, R. G. (1997). Caspase cleavage of keratin 18 and reorganization of intermediate filaments during epithelial cell apoptosis. *J. Cell Biol.* **138**, 1379-1394.

Charras, G. T., Yarrow, J. C., Horton, M. A., Mahadevan, L. and Mitchison, T. J. (2005). Non-equilibration of hydrostatic pressure in blebbing cells. *Nature* **435**, 365-369.

Chen, F., Chang, R., Trivedi, M., Capetanaki, Y. and Cryns, V. L. (2003). Caspase proteolysis of desmin produces a dominant-negative inhibitor of intermediate filaments and promotes apoptosis. *J. Biol. Chem.* **278**, 6848-6853.

Clarke, M. C., Savill, J., Jones, D. B., Noble, B. S. and Brown, S. B. (2003). Compartmentalized megakaryocyte death generates functional platelets committed to caspase-independent death. *J. Cell Biol.* **160**, 577-587.

Cline, A. M. and Radic, M. Z. (2004). Murine lupus autoantibodies identify distinct subsets of apoptotic bodies. *Autoimmunity* **37**, 85-93.

Coleman, M. L., Sahai, E. A., Yeo, M., Bosch, M., Dewar, A. and Olson, M. F. (2001). Membrane blebbing during apoptosis results from caspase-mediated activation of ROCK I. *Nat. Cell Biol.* **3**, 339-345.

Cotter, T. G., Lennon, S. V., Glynn, J. M. and Green, D. R. (1992). Microfilament-disrupting agents prevent the formation of apoptotic bodies in tumor cells undergoing apoptosis. *Cancer Res.* **52**, 997-1005.

Croft, D. R., Coleman, M. L., Li, S., Robertson, D., Sullivan, T., Stewart, C. L. and Olson, M. F. (2005). Actin-myosin-based contraction is responsible for apoptotic nuclear disintegration. *J. Cell Biol.* **168**, 245-255.

De Botton, S., Sabri, S., Daugas, E., Zermati, Y., Guidotti, J. E., Hermine, O., Kroemer, G., Vainchenker, W. and Debili, N. (2002). Platelet formation is the consequence of caspase activation within megakaryocytes. *Blood* **100**, 1310-1317.

Fadok, V. A., Voelker, D. R., Campbell, P. A., Cohen, J. J., Bratton, D. L. and Henson, P. M. (1992). Exposure of phosphatidylserine on the surface of apoptotic lymphocytes triggers specific recognition and removal by macrophages. *J. Immunol.* **148**, 2207-2216.

Fadok, V. A., Bratton, D. L., Rose, D. M., Pearson, A., Ezekewitz, R. A. and Henson, P. M. (2000). A receptor for phosphatidylserine-specific clearance of apoptotic cells. *Nature* **405**, 85-90.

Fischer, U., Janicke, R. U. and Schulze-Osthoff, K. (2003). Many cuts to ruin: a comprehensive update of caspase substrates. *Cell Death Differ.* **10**, 76-100.

Gerner, C., Frohwein, U., Gotzmann, J., Bayer, E., Gelbmann, D., Bursch, W. and Schulte-Hermann, R. (2000). The Fas-induced apoptosis analyzed by high throughput proteome analysis. *J. Biol. Chem.* **275**, 39018-39026.

Hartwig, J. and Italiano, J., Jr (2003). The birth of the platelet. *J. Thromb. Haemost.* **1**, 1580-1586.

Hoffmann, P. R., deCathelineau, A. M., Ogden, C. A., Leverrier, Y., Bratton, D. L., Daleke, D. L., Ridley, A. J., Fadok, V. A. and Henson, P. M. (2001). Phosphatidylserine (PS) induces PS receptor-mediated macropinocytosis and promotes clearance of apoptotic cells. *J. Cell Biol.* **155**, 649-659.

Italiano, J. E., Jr, Lecine, P., Shivdasani, R. A. and Hartwig, J. H. (1999). Blood platelets are assembled principally at the ends of proplatelet processes produced by differentiated megakaryocytes. *J. Cell Biol.* **147**, 1299-1312.

Kerr, J. F., Wyllie, A. H. and Currie, A. R. (1972). Apoptosis: a basic biological phenomenon with wide-ranging implications in tissue kinetics. *Br. J. Cancer* **26**, 239-257.

Lane, J. and Allan, V. (1998). Microtubule-based membrane movement. *Biochim. Biophys. Acta* **1376**, 27-55.

Lane, J. D., Vergnolle, M. A., Woodman, P. G. and Allan, V. J. (2001). Apoptotic cleavage of cytoplasmic dynein intermediate chain and p150(Glued) stops dynein-dependent membrane motility. *J. Cell Biol.* **153**, 1415-1426.

Lane, J. D., Lucocq, J., Pryde, J., Barr, F. A., Woodman, P. G., Allan, V. J. and Lowe, M. (2002). Caspase-mediated cleavage of the stacking protein GRASP65 is required for Golgi fragmentation during apoptosis. *J. Cell Biol.* **156**, 495-509.

Lane, J. D., Allan, V. J. and Woodman, P. G. (2005). Active relocation of chromatin and endoplasmic reticulum into blebs in late apoptotic cells. *J. Cell Sci.* **118**, 4059-4071.

Lecine, P., Italiano, J. E., Jr, Kim, S. W., Villeval, J. L. and Shivdasani, R. A. (2000). Hematopoietic-specific beta 1 tubulin participates in a pathway of platelet biogenesis dependent on the transcription factor NF-E2. *Blood* **96**, 1366-1373.

Leist, M. and Jaattela, M. (2001). Four deaths and a funeral: from caspases to alternative mechanisms. *Nat. Rev. Mol. Cell Biol.* **2**, 589-598.

Lowe, M., Lane, J. D., Woodman, P. G. and Allan, V. J. (2004). Caspase-mediated cleavage of syntaxin 5 and giantin accompanies inhibition of secretory traffic during apoptosis. *J. Cell Sci.* **117**, 1139-1150.

Martin, S. J., Finucane, D. M., Amarante-Mendes, G. P., O'Brien, G. A. and Green, D. R. (1996). Phosphatidylserine externalization during CD95-induced apoptosis of cells and cytoplasts requires ICE/CED-3 protease activity. *J. Biol. Chem.* **271**, 28753-28756.

Maruta, H., Greer, K. and Rosenbaum, J. L. (1986). The acetylation of alpha-tubulin and its relationship to the assembly and disassembly of microtubules. *J. Cell Biol.* **103**, 571-579.

Mills, J. C., Lee, V. M. and Pittman, R. N. (1998a). Activation of a PP2A-like phosphatase and dephosphorylation of tau protein characterize onset of the execution phase of apoptosis. *J. Cell Sci.* **111**, 625-636.

Mills, J. C., Stone, N. L., Erhardt, J. and Pittman, R. N. (1998b). Apoptotic membrane blebbing is regulated by myosin light chain phosphorylation. *J. Cell Biol.* **140**, 627-636.

Mills, J. C., Stone, N. L. and Pittman, R. N. (1999). Extranuclear apoptosis. The role of the cytoplasm in the execution phase. *J. Cell Biol.* **146**, 703-708.

Morrison, E. E., Wardleworth, B. N., Askham, J. M., Markham, A. F. and Meredith, D. M. (1998). EB1, a protein which interacts with the APC tumour suppressor, is associated with the microtubule cytoskeleton throughout the cell cycle. *Oncogene* **17**, 3471-3477.

Morrison, E. E., Moncur, P. M. and Askham, J. M. (2002). EB1 identifies sites of

microtubule polymerisation during neurite development. *Brain Res. Mol. Brain Res.* **98**, 145-152.

Ogden, C. A., deCathelineau, A., Hoffmann, P. R., Bratton, D., Ghebrehiwet, B., Fadok, V. A. and Henson, P. M. (2001). C1q and mannose binding lectin engagement of cell surface calreticulin and CD91 initiates macropinocytosis and uptake of apoptotic cells. *J. Exp. Med.* **194**, 781-795.

Palazzo, A. F., Cook, T. A., Alberts, A. S. and Gundersen, G. G. (2001). mDia mediates Rho-regulated formation and orientation of stable microtubules. *Nat. Cell Biol.* **3**, 723-729.

Pittman, S. M., Strickland, D. and Ireland, C. M. (1994). Polymerization of tubulin in apoptotic cells is not cell cycle dependent. *Exp. Cell Res.* **215**, 263-272.

Pittman, S., Geyp, M., Fraser, M., Ellem, K., Peaston, A. and Ireland, C. (1997). Multiple centrosomal microtubule organising centres and increased microtubule stability are early features of VP-16-induced apoptosis in CCRF-CEM cells. *Leuk. Res.* **21**, 491-499.

Rao, L., Perez, D. and White, E. (1996). Lamin proteolysis facilitates nuclear events during apoptosis. *J. Cell Biol.* **135**, 1441-1455.

Rodriguez, O. C., Schaefer, A. W., Mandato, C. A., Forscher, P., Bement, W. M. and Waterman-Storer, C. M. (2003). Conserved microtubule-actin interactions in cell movement and morphogenesis. *Nat. Cell Biol.* **5**, 599-609.

Rosen, A. and Casciola-Rosen, L. (2001). Clearing the way to mechanisms of autoimmunity. *Nat. Med.* **7**, 664-665.

Ruchaud, S., Korfali, N., Villa, P., Kottke, T. J., Dingwall, C., Kaufmann, S. H. and Earnshaw, W. C. (2002). Caspase-6 gene disruption reveals a requirement for lamin A cleavage in apoptotic chromatin condensation. *EMBO J.* **21**, 1967-1977.

Savill, J. and Fadok, V. (2000). Corpse clearance defines the meaning of cell death. *Nature* **407**, 784-788.

Savill, J., Dransfield, I., Gregory, C. and Haslett, C. (2002). A blast from the past: clearance of apoptotic cells regulates immune responses. *Nat. Rev. Immunol.* **2**, 965-975.

Sebbagh, M., Renvoize, C., Hamelin, J., Riche, N., Bertoglio, J. and Breard, J. (2001). Caspase-3-mediated cleavage of ROCK I induces MLC phosphorylation and apoptotic membrane blebbing. *Nat. Cell Biol.* **3**, 346-352.

Sesso, A., Fujiwara, D. T., Jaeger, M., Jaeger, R., Li, T. C., Monteiro, M. M., Correa, H., Ferreira, M. A., Schumacher, R. I., Belisario, J. et al. (1999). Structural elements common to mitosis and apoptosis. *Tissue Cell* **31**, 357-371.

Straight, A. F., Cheung, A., Limouze, J., Chen, I., Westwood, N. J., Sellers, J. R. and Mitchison, T. J. (2003). Dissecting temporal and spatial control of cytokinesis with a myosin II inhibitor. *Science* **299**, 1743-1747.

Strasser, A., O'Connor, L. and Dixit, V. M. (2000). Apoptosis signaling. *Annu. Rev. Biochem.* **69**, 217-245.

Su, L. K., Burrell, M., Hill, D. E., Gyuris, J., Brent, R., Wiltshire, R., Trent, J., Vogelstein, B. and Kinzler, K. W. (1995). APC binds to the novel protein EB1. *Cancer Res.* **55**, 2972-2977.

White, R. A., Pan, Z. and Salisbury, J. L. (2000). GFP-centrin as a marker for centriole dynamics in living cells. *Microsc. Res. Tech.* **49**, 451-457.

White, S. and Rosen, A. (2003). Apoptosis in systemic lupus erythematosus. *Curr. Opin. Rheumatol.* **15**, 557-562.

Wittmann, T., Bokoch, G. M. and Waterman-Storer, C. M. (2003). Regulation of leading edge microtubule and actin dynamics downstream of Rac1. *J. Cell Biol.* **161**, 845-851.

Young, A., Dictenberg, J. B., Purohit, A., Tuft, R. and Doxsey, S. J. (2000). Cytoplasmic dynein-mediated assembly of pericentrin and gamma tubulin onto centrosomes. *Mol. Biol. Cell* **11**, 2047-2056.